Implementing a cross-Kerr interaction between microwave and optical cavities and its application in generating a hybrid continuous-variable–discrete-variable entangled state

Jin Xu [1,2] and Tong Liu [1,*]

[1] *Quantum Information Research Center, Shangrao Normal University, Shangrao 334001, China*
[2] *School of Physics and Electronic Information, Shangrao Normal University, Shangrao 334001, China*

(Received 29 September 2023; revised 30 January 2024; accepted 20 February 2024; published 7 March 2024)

Microwave-optical interactions and hybrid entangled states are crucial for building hybrid quantum networks. In this work, we propose an approach for realizing a cross-Kerr nonlinear interaction between microwave and optical cavities using an ensemble of nitrogen-vacancy centers (NV ensemble). This cross-Kerr interaction is achieved by an NV ensemble dispersively coupled to a microwave cavity and an optical cavity. As an application, we show that the cross-Kerr interaction can be used to create a hybrid entangled state of a discrete-variable (DV) optical qubit and a continuous-variable (CV) optical qubit. The DV optical qubit here refers to a qubit, with two logic states encoded via the vacuum and single-photon states of the optical cavity. The CV optical qubit means a qubit, whose two logic states are encoded through two quasi-orthogonal coherent states or cat states of the microwave cavity. Our method is quite simple because it only requires a single-step operation. Numerical simulations demonstrate that high-fidelity generation of the proposed hybrid state is feasible within current experimental technology. This proposal is universal and the NV ensemble can be replaced by other quantum transducers, such as magnons, rare-earth-doped crystals, and silicon-vacancy centers.

DOI: 10.1103/PhysRevA.109.033705

I. INTRODUCTION

Hybrid quantum systems composed of two or more different physical systems (e.g., superconducting devices, atoms, optical cavities, ensembles of solid-state spins, etc.) have emerged as a promising platform for realizing quantum information processing (QIP) and quantum computing [1–3]. A hybrid system encompassing a superconducting microwave cavity, an optical cavity, and an NV ensemble is a type of hybrid quantum system. It combines the advantages of each physical subsystem. For example, microwave photons can be easily manipulated, while optical photons can be transferred by optical fibers, allowing long-distance QIP and quantum communication. The NV ensemble can be regarded as a good quantum memory since it has a long coherence time. Due to NV ensemble coupling to both microwave and optical cavities, it can act as a quantum transducer or quantum data bus between the microwave and optical photon domains [4–6]. To date, it has been experimentally demonstrated that there is a strong coupling between an NV ensemble and a superconducting cavity [7–10] or between an NV ensemble and an optical cavity [11–14]. It has also been demonstrated that there is a strong coupling of an NV ensemble with a superconducting qubit [15]. During the past decade, a great deal of theoretical proposals have been presented to implement various QIP tasks with NV ensembles [16–29].

Cross-Kerr nonlinearity plays a central role in quantum information science and technology. It has a wide range of applications in quantum information processing and quantum computation, such as quantum teleportation [30], quantum-nondemolition measurements [31], purification of entangled states [32], construction of the two-cavity qubits controlled-phase gate [33], preparation of the two-cavity macroscopic entangled coherent state [34], generation of the Gottesman-Kitaev-Preskill qubit [35]. Theoretically, many proposals have been presented for achieving the cross-Kerr nonlinearity in a variety of systems, including atoms [36,37], ions [38], optomechanical systems [39,40], cavity QED [41,42], superconducting circuits [34,43,44], etc. Experimentally, the cross-Kerr nonlinearity has been observed in Rydberg atoms [45,46], superconducting circuits [47–49], ions [50], and cavity magnonics [51]. However, a detailed proposal for realizing a cross-Kerr nonlinearity between microwave and optical cavities has not been put forward.

On the other hand, hybrid entangled states of discrete-variable (DV) qubits and continuous-variable (CV) qubits have drawn much attention recently. They are key resources in the hybrid quantum computation, the building up of hybrid quantum networks, and the linking of quantum processors with different encoding qubits [52,53]. During the past years, theoretical proposals have been made for preparing hybrid entangled states of DV optical qubits and CV optical qubits in linear optical systems [54,55] and superconducting circuits [56,57]. Moreover, hybrid entangled states of a DV optical qubit and a CV optical qubit have been experimentally prepared in linear optical systems [58–60]. The hybrid DV-CV entangled states have many applications in quantum repeaters and quantum computing [53,58,59].

In this work, we propose an approach to realize a cross-Kerr interaction between microwave and optical cavities by coupling an ensemble of NV centers. We find that this

*liutong7500755@163.com

cross-Kerr interaction can allow the preparation of a hybrid entangled state of a DV optical qubit and a CV optical qubit. The DV optical qubit here refers to a qubit with two logic states encoded through the vacuum and single-photon states of the optical cavity, while the CV optical qubit refers to a qubit with two logic states encoded via two quasi-orthogonal coherent states or cat states of the microwave cavity. We also show that the cross-Kerr interaction can be utilized to construct a hybrid two photonic qubits controlled phase gate, enabling the transfer of quantum states between the microwave and optical cavities. This proposal has the following advantages. (i) Due to the fact that the NV ensemble is not populated during the operation, the decoherence from the NV ensemble is greatly minimized. (ii) Our proposal is implemented using only a single-step operation. (iii) Because only a coupler NV ensemble is required, the architecture of the system is compact and simple. (iv) The generated hybrid entangled state is especially useful for long-distance quantum communication and QIP. (v) This proposal is general and can be applied to other quantum transducers such as magnons in a ferromagnetic material [51,61], rare-earth-doped crystals [62,63], and silicon-vacancy (SiV) centers in diamond [64], etc. To the best of our knowledge, a cross-Kerr nonlinear interaction has not been implemented before between microwave and optical cavities. The paper is organized as follows. In Sec. II, we introduce the hybrid system and give a derivation of the cross-Kerr interaction Hamiltonian between microwave and optical cavities. In Sec. III, as an application, we show that this cross-Kerr interaction Hamiltonian can be employed to prepare a hybrid entangled state of a DV optical qubit and a CV optical qubit. In Sec. IV, we further show that the cross-Kerr interaction Hamiltonian can be used to realize a hybrid two photonic qubits controlled phase gate. In Sec. V, we show how to transfer an arbitrary quantum state between microwave and optical cavities by utilizing the cross-Kerr interaction. In Sec. VI, we investigate the experimental feasibility of our proposal. A brief concluding summary is given in Sec. VII.

II. REALIZATION OF CROSS-KERR INTERACTION BETWEEN MICROWAVE AND OPTICAL CAVITIES

We consider a hybrid system schematically shown in Fig. 1(a), where an ensemble of NV centers is dispersively coupled to both an optical cavity and a planar superconducting microwave cavity.

An NV center in the diamond consists of a substitutional nitrogen atom and an adjacent vacancy. The ground state of the NV center is an electronic spin triplet state $|^3A_2\rangle = |E_0\rangle|m_s = 0, \pm 1\rangle$, where $|E_0\rangle$ is the orbital state with zero angular-momentum projection along the NV axis. There exists a 2.88-GHz zero-field splitting between the $|m_s = 0\rangle$ and $|m_s = \pm 1\rangle$ levels. By applying an extra magnetic field, the degeneracy of the levels $|m_s = +1\rangle$ and $|m_s = -1\rangle$ can be further split [Fig. 1(b)] [1]. We choose the coupling of the microwave cavity with the $|E_0\rangle|m_s = 0\rangle \leftrightarrow |E_0\rangle|m_s = +1\rangle$ transition of each NV center, while decoupling the microwave cavity from the $|E_0\rangle|m_s = 0\rangle \leftrightarrow |E_0\rangle|m_s = -1\rangle$ transition. The optical excited state is defined as $|A_2\rangle = \frac{1}{\sqrt{2}}(|E_-\rangle|m_s = +1\rangle + |E_+\rangle|m_s = -1\rangle)$ [4,5,65], where $|E_+\rangle$ ($|E_-\rangle$) is the orbital state with angular-momentum projection $+1$ (-1) along the NV axis. Typically, an NV center can be regarded as a spin while an ensemble of NV centers can be treated as a spin ensemble. The ground and the excited states of spin j ($j = 1, 2, 3, \ldots, N$) in the ensemble are labeled by $|0\rangle_j = |E_0\rangle|m_s = 0\rangle_j$, $|1\rangle_j = |E_0\rangle|m_s = +1\rangle_j$, and $|2\rangle_j = |A_2\rangle_j$, where N is the total number of the spins in the NV ensemble.

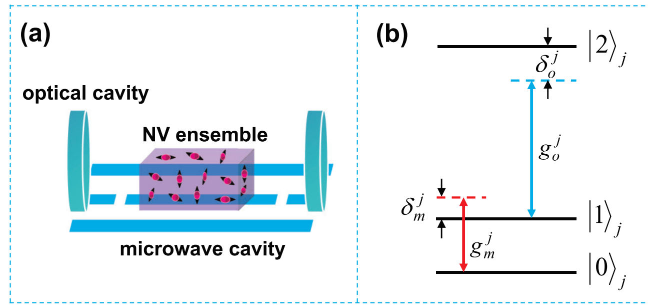

FIG. 1. (a) Diagram of a hybrid system consisting of an NV ensemble, an optical cavity and a planar superconducting microwave cavity. (b) Schematic diagram of the energy levels of NV center j. Microwave cavity is dispersively coupled to the $|0\rangle_j \leftrightarrow |1\rangle_j$ transition of NV center j with the coupling strength g_m^j and detuning $\delta_m^j < 0$, while the optical cavity is dispersively coupled to the $|1\rangle_j \leftrightarrow |2\rangle_j$ transition of NV center j with the coupling strength g_o^j and detuning $\delta_o^j > 0$.

As illustrated in Fig. 1(b), microwave cavity is dispersively coupled to the $|0\rangle_j \leftrightarrow |1\rangle_j$ transition of spin j in the ensemble, while optical cavity is dispersively coupled to the $|1\rangle_j \leftrightarrow |2\rangle_2$ transition of spin j ($j = 1, 2, 3, \ldots, N$). We introduce a coupling strength $g_m = (\sum_{j=1}^N |g_m^j|^2/N)^{1/2}$ [$g_o = (\sum_{j=1}^N |g_o^j|^2/N)^{1/2}$] to denote the average coupling strength for each spin of the ensemble, where g_m^j (g_o^j) is the coupling strength between the microwave cavity (optical cavity) and the $|0\rangle_j \leftrightarrow |1\rangle_j$ ($|1\rangle_j \leftrightarrow |2\rangle_j$) transition of the jth spin.

In the interaction picture and after making the rotating-wave approximation, the Hamiltonian of the system is given by (hereafter setting $\hbar = 1$)

$$H_{\rm I} = \sum_{j=1}^N g_m\left(\hat{a}^\dagger \tau_{10}^{j-} e^{-i\delta_m^j t} + \hat{a}\tau_{10}^{j+} e^{i\delta_m^j t}\right) + \sum_{j=1}^N g_o\left(\hat{b}^\dagger \tau_{21}^{j-} e^{-i\delta_o^j t} + \hat{b}\tau_{21}^{j+} e^{i\delta_o^j t}\right), \quad (1)$$

where $\hat{a}^\dagger$ and $\hat{a}$ ($\hat{b}^\dagger$ and $\hat{b}$) are the creation and the annihilation operators of the microwave (optical) cavity; $\tau_{10}^{j-} = |0\rangle_j\langle 1|$ ($\tau_{10}^{j+} = |1\rangle_j\langle 0|$) and $\tau_{21}^{j-} = |1\rangle_j\langle 2|$ ($\tau_{21}^{j+} = |2\rangle_j\langle 1|$) are the lowering (raising) operators of the jth spin for the ensemble; detunings $\delta_m^j = \omega_{10}^j - \omega_m < 0$ and $\delta_o^j = \omega_{21}^j - \omega_o > 0$. Here, ω_m (ω_o) is the frequency of the microwave (optical) cavity, while ω_{10}^j (ω_{21}^j) is the $|0\rangle_j \leftrightarrow |1\rangle_j$ ($|1\rangle_j \leftrightarrow |2\rangle_j$) transition frequency of the jth spin for the ensemble.

Since random distributions of spins may result in an inhomogeneous broadening of spin transition for an ensemble, we consider random shifts $\Delta_m^j = \delta_m^j - \delta_m$ and $\Delta_o^j = \delta_o^j - \delta_o$ for the jth spin of the ensemble [5,21]. Here, δ_m ($\delta_m < 0$)

and δ_o ($\delta_o > 0$) are the average detunings, respectively. Considering the large-detuning conditions $|\delta_m| \gg \{g_m, |\Delta_m^j|\}$ and $\delta_o \gg \{g_o, \Delta_o^j\}$, one can ignore the effect of inhomogeneous broadening of the transition frequencies for the ensemble in the following [5,21]. Then, one can obtain the effective Hamiltonian (see Appendix) [66–68]

$$\begin{aligned} H_e = &\sum_{j=1}^{N} -\frac{g_m^2}{\delta_m}(\hat{a}^\dagger\hat{a}|0\rangle_j\langle 0| - \hat{a}\hat{a}^\dagger|1\rangle_j\langle 1|) \\ &+\sum_{j=1}^{N}\frac{g_o^2}{\delta_o}(\hat{b}\hat{b}^\dagger|2\rangle_j\langle 2| - \hat{b}^\dagger\hat{b}|1\rangle_j\langle 1|) \\ &+\sum_{j=1}^{N}\lambda(\hat{a}^\dagger\hat{b}^\dagger|0\rangle_j\langle 2|e^{-i\delta_{om}t} + \hat{a}\hat{b}|2\rangle_j\langle 0|e^{i\delta_{om}t}), \end{aligned} \quad (2)$$

where $\lambda = (g_o g_m/2)(1/|\delta_m| + 1/\delta_o)$ and $\delta_{om} = \delta_o - |\delta_m|$. Under the large-detuning conditions, the indirect interaction between any two spins can be neglected. The first and second lines of Eq. (2) represent Stark shifts, the last line of Eq. (2) indicates the effective coupling among the microwave cavity, the optical cavity, and the $|0\rangle_j \leftrightarrow |2\rangle_j$ transition of the jth spin in ensemble.

Applying the large-detuning condition $|\delta_{om}| \gg \{\lambda, g_m^2/|\delta_m|, g_o^2/\delta_o\}$, the effective Hamiltonian (2) turns into (see Appendix) [66–68]

$$\begin{aligned} H_e = &\sum_{j=1}^{N} -\frac{g_m^2}{\delta_m}(\hat{a}^\dagger\hat{a}|0\rangle_j\langle 0| - \hat{a}\hat{a}^\dagger|1\rangle_j\langle 1|) \\ &+\sum_{j=1}^{N}\frac{g_o^2}{\delta_o}(\hat{b}\hat{b}^\dagger|2\rangle_j\langle 2| - \hat{b}^\dagger\hat{b}|1\rangle_j\langle 1|) \\ &+\sum_{j=1}^{N}\frac{\lambda^2}{\delta_{om}}(\hat{a}\hat{a}^\dagger\hat{b}\hat{b}^\dagger|2\rangle_j\langle 2| - \hat{a}^\dagger\hat{a}\hat{b}^\dagger\hat{b}|0\rangle_j\langle 0|). \end{aligned} \quad (3)$$

When the jth spin is in the ground state, the effective Hamiltonian (3) reduces to

$$H_e = -\sum_{j=1}^{N}\frac{g_m^2}{\delta_m}\hat{a}^\dagger\hat{a}|0\rangle_j\langle 0| - \sum_{j=1}^{N}\frac{\lambda^2}{\delta_{om}}\hat{a}^\dagger\hat{a}\hat{b}^\dagger\hat{b}|0\rangle_j\langle 0|. \quad (4)$$

Under the conditions of the weak excitations and the large N, one can express the spin operators in terms of the bosonic operators by utilizing the Holstein-Primakoff transformation [69,70]:

$$\begin{aligned} \sum_{j=1}^{N}\tau_{10}^{j-} &= \hat{c}\sqrt{N - \hat{c}^\dagger\hat{c}} \simeq \sqrt{N}\hat{c}, \\ \sum_{j=1}^{N}\tau_{10}^{j+} &= \hat{c}^\dagger\sqrt{N - \hat{c}^\dagger\hat{c}} \simeq \sqrt{N}\hat{c}^\dagger, \end{aligned} \quad (5)$$

where $\hat{c}^\dagger$ and $\hat{c}$ are bosonic operators which approximately obey the boson commutation relation $[\hat{c}, \hat{c}^\dagger] = 1 - \frac{2}{N}\hat{c}^\dagger\hat{c} \approx 1$ [71].

From Eqs. (5), one can obtain $\sum_{j=1}^{N}|0\rangle_j\langle 0| = \sum_{j=1}^{N}\tau_{10}^{j-}\tau_{10}^{j+} \simeq N\hat{c}\hat{c}^\dagger$. Thus, Eq. (4) can be further rewritten as

$$H_e = -\lambda_m\hat{a}^\dagger\hat{a} - \chi\hat{a}^\dagger\hat{a}\hat{b}^\dagger\hat{b}, \quad (6)$$

where $\lambda_m = (\sqrt{N}g_m)^2/\delta_m$ and $\chi = (\sqrt{N}\lambda)^2/\delta_{om}$. Here the degree of freedom of the ensemble has been eliminated because we assume that the spin ensemble is in the ground state.

In a rotating frame under the Hamiltonian $H_0 = -\lambda_m\hat{a}^\dagger\hat{a}$, we obtain

$$H_e = -\chi\hat{a}^\dagger\hat{a}\hat{b}^\dagger\hat{b}. \quad (7)$$

This effective Hamiltonian describes the cross-Kerr interaction between the microwave cavity and the optical cavity with coefficient χ. It is well known that the cross-Kerr nonlinearity has many important applications in QIP, quantum computing, and quantum communication [30–35]. In the next section, we discuss how to use the Hamiltonian (7) to prepare a hybrid entangled state of a DV optical qubit and a CV optical qubit.

III. CREATION OF ENTANGLEMENT BETWEEN DISCRETE-VARIABLE AND CONTINUOUS-VARIABLE OPTICAL QUBITS

In this section, we show that the cross-Kerr nonlinearity (7) can be used to prepare a hybrid entangled state between a DV optical qubit and a CV optical qubit. Assume that the microwave cavity is initially in a coherent state $|\alpha\rangle_a$ while the optical cavity is initially in a superposition state $(1/\sqrt{2})(|0\rangle_b + |1\rangle_b)$, where $|0\rangle_b$ and $|1\rangle_b$ are the vacuum state and the single-photon state of the optical cavity. Then we can obtain the following state evolution under the Hamiltonian (7):

$$\begin{aligned} &\frac{1}{\sqrt{2}}e^{i\chi\hat{a}^\dagger\hat{a}\hat{b}^\dagger\hat{b}t}|\alpha\rangle_a(|0\rangle_b + |1\rangle_b) \\ &= \frac{1}{\sqrt{2}}e^{i\chi\hat{a}^\dagger\hat{a}\hat{b}^\dagger\hat{b}t}e^{-\frac{1}{2}|\alpha|^2}\sum_{n_a=0}^{\infty}\frac{\alpha^{n_a}}{\sqrt{n_a!}}|n_a\rangle_a(|0\rangle_b + |1\rangle_b) \\ &= \frac{1}{\sqrt{2}}\left(|\alpha\rangle_a|0\rangle_b + e^{-\frac{1}{2}|\alpha|^2}\sum_{n_a=0}^{\infty}\frac{\alpha^{n_a}e^{i\chi\hat{n}_a\hat{n}_b t}}{\sqrt{n_a!}}|n_a\rangle_a|1\rangle_b\right) \\ &= \frac{1}{\sqrt{2}}(|\alpha\rangle_a|0\rangle_b + |\alpha e^{i\chi t}\rangle_a|1\rangle_b), \end{aligned} \quad (8)$$

where $\hat{n}_a = \hat{a}^\dagger\hat{a}$ and $\hat{n}_b = \hat{b}^\dagger\hat{b}$ are the photon number operators of the microwave and optical cavities, respectively.

At the evolution time $t = \pi/|\chi|$, the state (8) turns into

$$\frac{1}{\sqrt{2}}(|\alpha\rangle_a|0\rangle_b + |-\alpha\rangle_a|1\rangle_b), \quad (9)$$

which shows that a hybrid entangled state between a CV optical qubit and a DV optical qubit is created. Here, the two logic states of the CV qubit are encoded with the two coherent states $|\alpha\rangle_a$ and $|-\alpha\rangle_a$ of the microwave cavity, while the two logic states of the DV qubit are encoded with the vacuum state $|0\rangle_b$ and the single-photon state $|1\rangle_b$ of the optical cavity. Note that the hybrid entangled state (9) has already been experimentally generated in linear optical systems [58–60]. While, we here focus on its implementation in a microwave-optical hybrid system, i.e., a system completely different from the linear optical system.

Under the condition $|\lambda_m|t = 2k\pi$ (k is a positive integer) and after returning to the original interaction picture by applying a unitary transformation $U = e^{-iH_0 t}$, one can find that the hybrid entangled state (9) is unchanged. According to the conditions $t = \pi/|\chi|$ and $|\lambda_m|t = 2k\pi$, we have

$$\sqrt{N}g_o = \frac{|\delta_0|}{|\delta_m| + |\delta_o|}\sqrt{\frac{2|\delta_{om}\delta_m|}{k}}. \tag{10}$$

We perform a $|0\rangle_b \rightarrow |+\rangle_b$ and $|1\rangle_b \rightarrow |-\rangle_b$ rotation on the DV qubit, where $|+\rangle = (|0\rangle_b + |1\rangle_b)/\sqrt{2}$ and $|-\rangle = (|1\rangle_b - |0\rangle_b)/\sqrt{2}$. Then, the state (9) becomes

$$\frac{1}{\sqrt{2}}(|\mathrm{cat}_-\rangle_\mathrm{a}|0\rangle_\mathrm{b} + |\mathrm{cat}_+\rangle_\mathrm{a}|1\rangle_\mathrm{b}), \tag{11}$$

where $|\mathrm{cat}_\pm\rangle_\mathrm{a} = (|\alpha\rangle_\mathrm{a} \pm |\alpha\rangle_\mathrm{a})/\sqrt{2}$ denotes an even or odd cat state. Equation (11) shows that a hybrid entangled state of the CV qubit (encoded in the cat states) and the DV qubit is prepared.

This method can be extended to generate a hybrid high-dimensional entangled state of a CV qudit and a DV qudit. Suppose that the optical cavity is initially in a superposition of Fock states $\frac{1}{\sqrt{d}}\sum_{n=0}^{d-1}|n\rangle_b$ with n photons. If the microwave cavity is initially in a coherent state $|\alpha\rangle_a$, under the Hamiltonian (7), one can obtain the state evolution

$$\frac{1}{\sqrt{d}}(|\alpha\rangle_a|0\rangle_b + |\alpha e^{i\varphi}\rangle_a|1\rangle_b + |\alpha e^{i2\varphi}\rangle_a|2\rangle_b + \cdots + |\alpha e^{in\varphi}\rangle_a|n\rangle_b), \tag{12}$$

where $\varphi = \chi t$.

If the microwave cavity is initially in a cat state $|\mathrm{cat}_+\rangle_\mathrm{a}$, under the Hamiltonian (7), one has

$$\frac{1}{\sqrt{d}}(|\mathrm{cat}_+^0\rangle_\mathrm{a}|0\rangle_\mathrm{b} + |\mathrm{cat}_+^1\rangle_\mathrm{a}|1\rangle_\mathrm{b} + |\mathrm{cat}_+^2\rangle_\mathrm{a}|2\rangle_\mathrm{b} + \cdots + |\mathrm{cat}_+^\mathrm{n}\rangle_\mathrm{a}|\mathrm{n}\rangle_\mathrm{b}), \tag{13}$$

where cat state $|\mathrm{cat}_+^\mathrm{n}\rangle_\mathrm{a} = (|\alpha \mathrm{e}^{\mathrm{i}n\varphi}\rangle_\mathrm{a} + |\alpha \mathrm{e}^{\mathrm{i}n\varphi}\rangle_\mathrm{a})/\sqrt{2}$ ($n = 0, 1, 2, \ldots, d-1$). Equations (12) and (13) display that a hybrid high-dimensional entangled state of a CV qudit and a DV qudit is created.

IV. IMPLEMENTATION OF A HYBRID CONTROLLED PHASE GATE OF MICROWAVE AND OPTICAL CAVITIES

We assume that the microwave and optical cavities are initially prepared in superposition states $|\psi\rangle_a = \frac{1}{\sqrt{2}}(|0\rangle_a + |1\rangle_a)$ and $|\psi\rangle_b = \frac{1}{\sqrt{2}}(|0\rangle_b + |1\rangle_b)$. Under the Hamiltonian (7), the time evolution operator is given by $U(t) = e^{-iH_e t}$. In the computational basis states $\{|0\rangle_a|0\rangle_b, |0\rangle_a|1\rangle_b, |1\rangle_a|0\rangle_b, |1\rangle_a|1\rangle_b\}$, one can obtain the following state transformation:

$$\begin{aligned}
U(t)|0\rangle_a|0\rangle_b &\rightarrow |0\rangle_a|0\rangle_b,\\
U(t)|0\rangle_a|1\rangle_b &\rightarrow |0\rangle_a|1\rangle_b,\\
U(t)|1\rangle_a|0\rangle_b &\rightarrow |1\rangle_a|0\rangle_b,\\
U(t)|1\rangle_a|1\rangle_b &\rightarrow e^{i\varphi}|1\rangle_a|1\rangle_b,
\end{aligned} \tag{14}$$

where $\varphi = \chi t$. After returning to the original interaction picture and satisfying the condition $|\lambda_m|t = 2k\pi$ (k is a positive integer), one can easily find that the transformation (14) is unchanged. Equations (14) shows that a hybrid two photonic qubits controlled phase gate of the microwave and optical cavities is realized. For $\varphi = \pi$, one can obtain $|1\rangle_a|1\rangle_b \rightarrow -|1\rangle_a|1\rangle_b$, which leads to a sign flip while other states remain unchanged.

Our approach is not limited to implementing controlled phase gates with discrete variable states, but it can also be used to realize controlled phase gates for arbitrary quantum state encodings. We use two arbitrary orthogonal states of a cavity to encode the two logic states $|\bar{0}\rangle$ and $|\bar{1}\rangle$ of a photonic qubit:

$$|\bar{0}\rangle = \sum_{n=\mathrm{even}}^{\infty} c_n|n\rangle, \quad |\bar{1}\rangle = \sum_{m=\mathrm{odd}}^{\infty} c_m|m\rangle, \tag{15}$$

where c_n and c_m are normalization coefficients.

Under Hamiltonian (7), one has

$$\begin{aligned}
U(t)|\bar{0}\rangle_a|\bar{0}\rangle_b &= \sum_{n,n'} e^{inn'\chi t} c_n c_{n'}|n\rangle_a|n'\rangle_b,\\
U(t)|\bar{0}\rangle_a|\bar{1}\rangle_b &= \sum_{n,m'} e^{inm'\chi t} c_n c_{m'}|n\rangle_a|m'\rangle_b,\\
U(t)|\bar{1}\rangle_a|\bar{0}\rangle_b &= \sum_{m,n'} e^{imn'\chi t} c_m c_{n'}|m\rangle_a|n'\rangle_b,\\
U(t)|\bar{1}\rangle_a|\bar{1}\rangle_b &= \sum_{m,m'} e^{imm'\chi t} c_m c_{m'}|m\rangle_a|m'\rangle_b,
\end{aligned} \tag{16}$$

where n and n' are even numbers, while m and m' are odd numbers. For $\chi t = \pi$, one can obtain $e^{inn'\chi t} = e^{inm'\chi t} = e^{imn'\chi t} = 1$, and $e^{imm'\chi t} = -1$. Thus, from Eqs. (16), one can obtain the state transformation

$$\begin{aligned}
U(t)|\bar{0}\rangle_a|\bar{0}\rangle_b &\rightarrow |\bar{0}\rangle_a|\bar{0}\rangle_b,\\
U(t)|\bar{0}\rangle_a|\bar{1}\rangle_b &\rightarrow |\bar{0}\rangle_a|\bar{1}\rangle_b,\\
U(t)|\bar{1}\rangle_a|\bar{0}\rangle_b &\rightarrow |\bar{1}\rangle_a|\bar{0}\rangle_b,\\
U(t)|\bar{1}\rangle_a|\bar{1}\rangle_b &\rightarrow -|\bar{1}\rangle_a|\bar{1}\rangle_b,
\end{aligned} \tag{17}$$

which results in a sign flip if and only if the two cavities are in the state $|\bar{1}\rangle_a|\bar{1}\rangle_b$. Thus, one can construct a hybrid controlled phase gate using two photonic qubits encoded in optical and microwave cavities with arbitrary states $|\bar{0}\rangle$ and $|\bar{1}\rangle$. Notice that the states $|\bar{0}\rangle$ and $|\bar{1}\rangle$ can be discrete-variable states (e.g., Fock state) or continuous-variable states (e.g., cat state). For example, if the microwave cavity is encoded by the cat states $|\mathrm{cat}_+\rangle_\mathrm{a}$ and $|\mathrm{cat}_-\rangle_\mathrm{a}$, and the optical cavity is encoded by the vacuum state $|0\rangle_b$ and the single-photon state $|1\rangle_b$, one can implement a hybrid CV-DV controlled phase gate according to Eqs. (17). The controlled phase gate is widely used in various quantum applications, including quantum error correction, quantum algorithms, quantum cloning, and quantum entanglement preparation, etc.

V. TRANSFER OF QUANTUM STATES BETWEEN THE MICROWAVE AND OPTICAL CAVITIES

Suppose that the initial states of the microwave and optical cavities are $|\psi\rangle_a = \sin\theta|0\rangle_a + \cos\theta|1\rangle_a$ and $|\psi\rangle_b = |0\rangle_b$, respectively. Here, $\sin\theta$ and $\cos\theta$ are normalization coefficients. We apply a Hadamard gate operation to the optical cavity such that $|0\rangle_b \to |+\rangle_b$ with $|+\rangle = (|0\rangle_b + |1\rangle_b)/\sqrt{2}$. Thus, the initial state of the microwave and optical cavities becomes

$$\frac{1}{\sqrt{2}}(\sin\theta|0\rangle_a|0\rangle_b + \sin\theta|0\rangle_a|1\rangle_b + \cos\theta|1\rangle_a|0\rangle_b + \cos\theta|1\rangle_a|1\rangle_b). \tag{18}$$

Then we perform a hybrid controlled phase gate operation on the microwave and optical cavities. From gate (14) with $\varphi = \pi$, one can see that the state (18) changes as

$$\frac{1}{\sqrt{2}}(\sin\theta|0\rangle_a|0\rangle_b + \sin\theta|0\rangle_a|1\rangle_b + \cos\theta|1\rangle_a|0\rangle_b - \cos\theta|1\rangle_a|1\rangle_b). \tag{19}$$

By performing two Hadamard gate operations on the microwave and optical cavities, one can realize $|0\rangle_a \to |+\rangle_a$, $|1\rangle_a \to |-\rangle_a$, $|+\rangle_b \to |0\rangle_b$, and $|1\rangle_b \to |-\rangle_b$. Thus, the state (19) turns into

$$\frac{1}{\sqrt{2}}[|0\rangle_a(\sin\theta|0\rangle_b + \cos\theta|1\rangle_b) + |1\rangle_a(\sin\theta|0\rangle_b - \cos\theta|1\rangle_b)]. \tag{20}$$

Now we perform a measurement on the microwave cavity. From Eq. (20), one can see that if the microwave cavity is measured in the state $|0\rangle_a$, an arbitrary state of the microwave cavity is fully transferred to the optical cavity. If the microwave cavity is measured in the state $|1\rangle_a$, after a σ_z gate operation applied to the optical cavity, the microwave cavity's state can be transferred to the optical cavity.

It is well known that microwave photons can be easily generated and manipulated, while optical photons can be transmitted over long distances via optical fibers. Equation (20) shows that an arbitrary quantum state of the microwave cavity has been transferred to the optical cavity, which is useful for quantum communication and quantum information processing in large-scale quantum networks.

VI. EXPERIMENTAL FEASIBILITY

After considering the dissipation of the NV ensemble, the microwave and optical cavities, the dynamics of the lossy system is described by using a Markovian master equation

$$\frac{d\rho}{dt} = -i[H_e, \rho] + \kappa_a\mathcal{D}[\hat{a}] + \kappa_b\mathcal{D}\big[\hat{b}\big] + \kappa_c\mathcal{D}[\hat{c}], \tag{21}$$

where ρ is the density matrix of the system; H_e is given by Eq. (4); $\mathcal{D}[\hat{O}] = (2\hat{O}\rho\hat{O}^\dagger - \hat{O}^\dagger\hat{O}\rho - \rho\hat{O}^\dagger\hat{O})/2$ (with $\hat{O} = \hat{a}, \hat{b}, \hat{c}$); κ_a, κ_b, and κ_c are, respectively, the decay rates of the microwave cavity, the optical cavity, and the NV ensemble.

By solving the Markovian master equation (21), we numerically calculate the operation fidelity for the hybrid DV-CV entangled state preparation. Part of numerical calculations are coded in Python by using the QuTiP library [72,73]. The fidelity of the operation can be calculated by $\mathcal{F} = \sqrt{\langle\psi_{\rm id}|\rho|\psi_{\rm id}\rangle}$, where $|\psi_{\rm id}\rangle$ is the ideal target state given by Eq. (9).

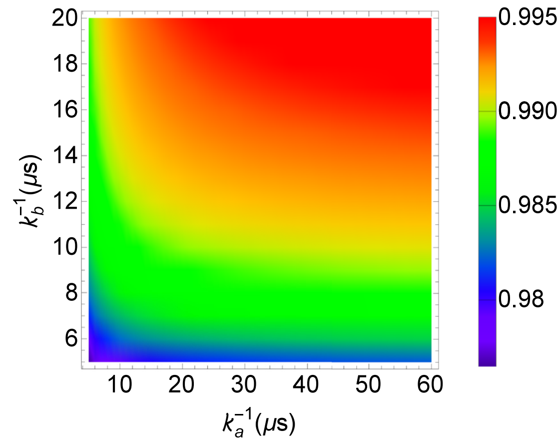

FIG. 2. Fidelity $\mathcal{F}$ versus κ_a^{-1} and κ_b^{-1} for the DV-CV entangled state. The values of the parameters in the numerical simulations are given in the main text.

We take NV ensemble-microwave cavity coupling strength $\sqrt{N}g_m/2\pi = 15$ MHz, where the total number of NV centers is $N \approx 10^{12}$ [7–10]. The detunings are chosen as $\delta_m/2\pi = -150$ MHz and $\delta_o/2\pi = 5.5$ GHz. According to Eq. (10), one has $\sqrt{N}g_o/2\pi \approx 551$ MHz. The value of $\sqrt{N}g_m$ ($\sqrt{N}g_o$) here is available in experiments since the coupling strength 3–17 MHz (0.3–1 GHz) between an NV ensemble and a planar superconducting microwave cavity [7–10] (an optical cavity [11–14]) has been experimentally demonstrated. In addition, we set the inhomogeneous broadening of the transition frequencies are $\Delta_m^j/2\pi = -10$ MHz and $\Delta_o^j/2\pi = 0.5$ GHz, which can be achieved with experimentally observed values of $|\Delta_m^j|/2\pi = 6$–12 MHz [10,74,75] and $\Delta_o^j/2\pi = 0.45$–20 GHz [76–78]. Thus, one can obtain $\delta_m^j/2\pi = -160$ MHz and $\delta_o^j/2\pi = 6.0$ GHz. The cross-Kerr coupling strength is $\chi/2\pi = 0.15$ MHz. Other parameters used in the numerical simulations are $\alpha = 0.5$, $k = 5$, and $\kappa_c/2\pi = 100$ kHz.

Figure 2 displays the fidelity $\mathcal{F}$ as a function of κ_a^{-1} and κ_b^{-1} for the hybrid DV-CV entangled state generation. From Fig. 2, one can see that for $\kappa_a^{-1} \geqslant 5$ μs and $\kappa_b^{-1} \geqslant 5$ μs, the fidelity can exceed 97.65%. When $\kappa_a^{-1} = 55$ μs and $\kappa_b^{-1} = 20$ μs, the fidelity is greater than 99.50%. In experiments, a planar superconducting microwave cavity with photon lifetimes ≈0.05–0.5 ms [79], an optical cavity with photon lifetimes ≈0.5–2.5 ms [80,81], and an NV ensemble with coherence times ≈0.3 ms to 1 s [82,83] have been reported. Moreover, the quality factors $Q_a \approx 10^6$–10^7 [79,84] and $Q_b \approx 10^{10}$–10^{12} [80,81,85,86] of the planar superconducting microwave and optical cavities have been respectively demonstrated in experiments.

To investigate the effect of the operation time errors on the fidelity, we set the actual operation time to be $(\epsilon + 1)t$, where t is the optimal operation time. Figure 3 shows the fidelity $\mathcal{F}$ versus ϵ, which is plotted by choosing $\kappa_a^{-1} = 55$ μs

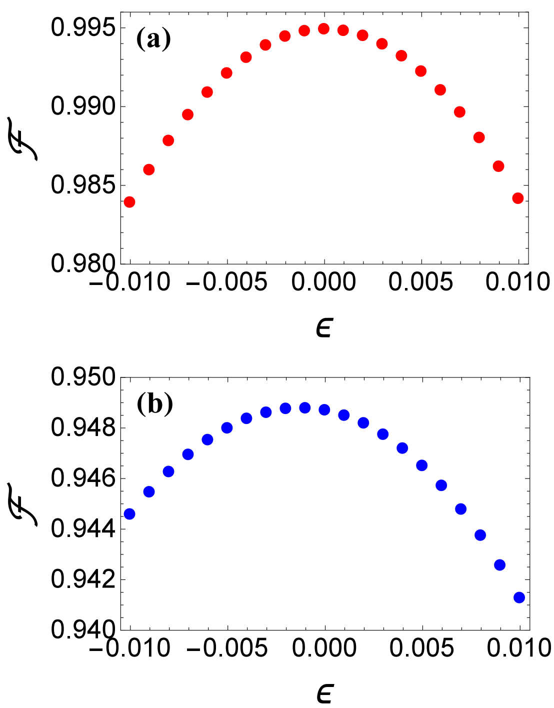

FIG. 3. Fidelity $\mathcal{F}$ versus ε by considering the effect of small operation time errors based on (a) the effective Hamiltonian and (b) the full Hamiltonian.

and $\kappa_b^{-1} = 20$ μs. In addition, other parameters used in the numerical simulation are the same as those used in Fig. 2. From Fig. 3(a), one can observe that when $\epsilon \in [-0.01, 0.01]$, the fidelity exceeds 98.40%. To validate the effectiveness of the made approximations, we numerically calculate the fidelity based on the full Hamiltonian (1). Because it is computationally expensive to simulate the full system Hamiltonian, we simulate the full Hamiltonian with time dependence on only a single term (i.e., $N = 1$) in Fig. 3(b). Figure 3(b) shows the fidelity surpasses 94.13% for $\epsilon \in [-0.01, 0.01]$. Thus, the hybrid DV-CV entangled state of the microwave and optical cavities can be high fidelity prepared for small operation time errors. From Figs. 3(a) and 3(b), it can be observed that, through numerical simulations comparing the effective Hamiltonian with the full Hamiltonian, the fidelity decreases by 4%–5%. This demonstrates the approximations made for the effective Hamiltonian are valid.

We then numerically calculate the fidelity of the hybrid controlled phase gate operation based on the effective Hamiltonian (4) and the full Hamiltonian (1). The initial state of cavity system is $(1/2)(|0\rangle_a + |1\rangle_a)(|0\rangle_b + |1\rangle_b)$, and the ideal target state is $(1/2)(|0\rangle_a|0\rangle_b + |0\rangle_a|1\rangle_b + |1\rangle_a|0\rangle_b - |1\rangle_a|1\rangle_b)$. We choose $\sqrt{N}g_m/2\pi \approx 12.7$ MHz and $k = 7$. Other parameters used in the numerical simulation are the same as those used in Fig. 3. Based on the effective Hamiltonian (4) and the full Hamiltonian (1), we calculate the fidelities are approximately 99.99% and 99.19% (98.70% and 95.59%) with (without) considering the systematic dissipation, respectively. Thus, the approximations made for the effective Hamiltonian are reasonable.

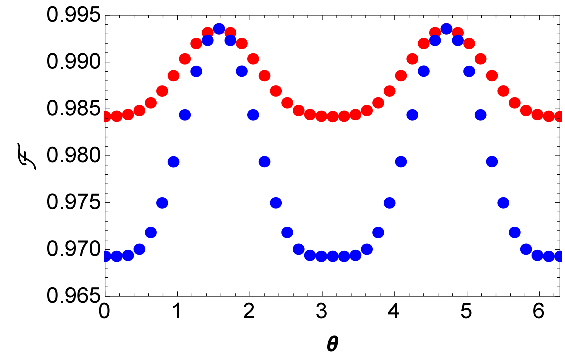

FIG. 4. Fidelity $\mathcal{F}$ versus θ for the state transfer. The red dots are based on the effective Hamiltonian while the blue dots are based on the full Hamiltonian.

By using the same parameters, we numerically calculate the fidelity of the state transfer operation based on the effective Hamiltonian (4) and the full Hamiltonian (1). The initial state is $(\sin\theta|0\rangle_a + \cos\theta|1\rangle_a)|0\rangle_b$, and the ideal target state is given by Eq. (20). Figure 4 shows the fidelity $\mathcal{F}$ versus θ ($\theta \in [0, 2\pi]$). The red and blue dots represent, respectively, the results obtained using the effective Hamiltonian (4) and the full Hamiltonian (1), taking into account the systematic dissipation. Figure 4 indicates that the fidelity based on the full Hamiltonian slightly decreased by 0.1%–1.5% compared with using the effective Hamiltonian. Moreover, it can be observed that an arbitrary state of the microwave cavity can be high-fidelity transferred to the optical cavity.

VII. CONCLUSION

We have proposed a method for realizing a cross-Kerr interaction between a microwave cavity and an optical cavity by using an ensemble of NV centers. We have shown that such a cross-Kerr interaction can be applied to create hybrid entanglement between discrete-variable and continuous-variable optical qubits, to construct a hybrid two photonic qubits controlled phase gate, and to transfer an arbitrary quantum state between the microwave and optical cavities. Since the NV ensemble is not excited during the operation, the decoherence from the NV ensemble is significantly suppressed. Due to the simplicity of our proposal, which requires only a coupler and a single-step operation, the experimental difficulty is reduced. Numerical simulations have further demonstrated that a hybrid continuous-variable–discrete-variable entangled state can be generated with high fidelity within the current experimental technology. Finally, this proposal is quite general and can be applied to a wide range of quantum transducers. Our finding may have many potential applications in large-scale hybrid QIP, hybrid quantum computation, and long-distance quantum communication.

ACKNOWLEDGMENTS

This work was partly supported by the National Natural Science Foundation of China (NSFC) (Grants No. 12364048 and No. 12004253), the Jiangxi Natural Science Foundation (Grant No. 20212BAB211019), the Jiangxi Education

Department Fund (Grant No. GJJ2201809), and the Innovation Program for Quantum Science and Technology (Grant No. 2021ZD0301704).

APPENDIX: DERIVATION OF THE EFFECTIVE HAMILTONIAN

In this Appendix, we derive the effective Hamiltonian (7) in the main text by employing the method [68]. In the interaction picture, the interaction Hamiltonian of the system has the form

$$\hat{H}_{\mathrm{I}}(t)=\sum_{n=1}^{N}\hat{h}_n\exp(-i\omega_n t)+\hat{h}_n^{+}\exp(i\omega_n t), \tag{A1}$$

where N is the total number different harmonic terms making up the interaction Hamiltonian, and the detuning $\omega_n>0$.

Under the large-detuning conditions, one can obtain a time-averaged effective Hamiltonian [68]

$$H_e=\sum_{m,n=1}^{N}\frac{1}{\overline{\omega}_{mn}}[\hat{h}_m^{+},\hat{h}_n]\exp[i(\omega_m-\omega_n)t], \tag{A2}$$

where $1/\overline{\omega}_{mn}=\frac{1}{2}(1/\omega_m+1/\omega_n)$.

In our main text, the interaction Hamiltonian of the system is given by Eq. (1), i.e.,

$$H_{\mathrm{I}}=\sum_{j=1}^{N}g_m\big(\hat{a}^{\dagger}\tau_{10}^{j-}e^{-i\delta_m^j t}+\hat{a}\tau_{10}^{j+}e^{i\delta_m^j t}\big)+\sum_{j=1}^{N}g_o\big(\hat{b}^{\dagger}\tau_{21}^{j-}e^{-i\delta_o^j t}+\hat{b}\tau_{21}^{j+}e^{i\delta_o^j t}\big), \tag{A3}$$

where detunings $\delta_m^j<0$ and $\delta_o^j>0$.

According to Eqs. (A1) and (A2), we choose $\hat{h}_1^{+}=\sum_{j=1}^{N}g_m\hat{a}^{\dagger}\tau_{10}^{j-}$, $\omega_1=-\delta_m^j$, $\hat{h}_2^{+}=\sum_{j=1}^{N}g_o\hat{b}\tau_{21}^{j+}$, and $\omega_2=\delta_o^j$. Then we introduce average detunings δ_m and δ_o, random shifts $\Delta_m^j=\delta_m^j-\delta_m$ and $\Delta_o^j=\delta_o^j-\delta_o$ for the jth spin of the ensemble [5,21]. In the dispersive regime $|\delta_m|\gg\{g_m,|\Delta_m^j|\}$ and $\delta_o\gg\{g_o,\Delta_o^j\}$, one can ignore the effect of inhomogeneous broadening of the transition frequencies for the ensemble in the following [5,21]. Thus, we have

$$\begin{aligned}
[\hat{h}_1^{+},\hat{h}_1]&=\sum_{j=1}^{N}g_m^2(\hat{a}^{\dagger}\hat{a}|0\rangle_j\langle 0|-\hat{a}\hat{a}^{\dagger}|1\rangle_j\langle 1|),\\
[\hat{h}_2^{+},\hat{h}_2]&=\sum_{j=1}^{N}g_o^2(\hat{b}\hat{b}^{\dagger}|2\rangle_j\langle 2|-\hat{b}^{\dagger}\hat{b}|1\rangle_j\langle 1|),\\
[\hat{h}_1^{+},\hat{h}_2]&=\sum_{j=1}^{N}g_m g_o\hat{a}^{\dagger}\hat{b}^{\dagger}|0\rangle_j\langle 2|,\\
[\hat{h}_2^{+},\hat{h}_1]&=\sum_{j=1}^{N}g_m g_o\hat{a}\hat{b}|2\rangle_j\langle 0|.
\end{aligned} \tag{A4}$$

By inserting Eq. (A4) into Eq. (A2), one can obtain the effective Hamiltonian

$$\begin{aligned}
H_e=&\sum_{j=1}^{N}-\frac{g_m^2}{\delta_m}(\hat{a}^{\dagger}\hat{a}|0\rangle_j\langle 0|-\hat{a}\hat{a}^{\dagger}|1\rangle_j\langle 1|)\\
&+\sum_{j=1}^{N}\frac{g_o^2}{\delta_o}(\hat{b}\hat{b}^{\dagger}|2\rangle_j\langle 2|-\hat{b}^{\dagger}\hat{b}|1\rangle_j\langle 1|)\\
&+\sum_{j=1}^{N}\lambda(\hat{a}^{\dagger}\hat{b}^{\dagger}|0\rangle_j\langle 2|e^{-i\delta_{om}t}+\hat{a}\hat{b}|2\rangle_j\langle 0|e^{i\delta_{om}t}),
\end{aligned} \tag{A5}$$

where $\lambda=(g_o g_m/2)(1/|\delta_m|+1/\delta_o)$ and $\delta_{om}=\delta_o-|\delta_m|$.

Then we choose $\hat{h}_3^{+}=\sum_{j=1}^{N}\lambda\hat{a}\hat{b}|2\rangle_j\langle 0|$ and $\omega_3=\delta_{om}>0$. One can obtain

$$[\hat{h}_3^{+},\hat{h}_3]=\sum_{j=1}^{N}\lambda^2(\hat{a}\hat{a}^{\dagger}\hat{b}\hat{b}^{\dagger}|2\rangle_j\langle 2|-\hat{a}^{\dagger}\hat{a}\hat{b}^{\dagger}\hat{b}|0\rangle_j\langle 0|). \tag{A6}$$

In the dispersive regime $\delta_{om}\gg\{\lambda,g_m^2/|\delta_m|,g_o^2/\delta_o\}$, and by inserting Eq. (A6) into the formula (A2), the Hamiltonian (A5) becomes

$$\begin{aligned}
H_e=&\sum_{j=1}^{N}-\frac{g_m^2}{\delta_m}(\hat{a}^{\dagger}\hat{a}|0\rangle_j\langle 0|-\hat{a}\hat{a}^{\dagger}|1\rangle_j\langle 1|)\\
&+\sum_{j=1}^{N}\frac{g_o^2}{\delta_o}(\hat{b}\hat{b}^{\dagger}|2\rangle_j\langle 2|-\hat{b}^{\dagger}\hat{b}|1\rangle_j\langle 1|)\\
&+\sum_{j=1}^{N}\frac{\lambda^2}{\delta_{om}}(\hat{a}\hat{a}^{\dagger}\hat{b}\hat{b}^{\dagger}|2\rangle_j\langle 2|-\hat{a}^{\dagger}\hat{a}\hat{b}^{\dagger}\hat{b}|0\rangle_j\langle 0|).
\end{aligned} \tag{A7}$$

If the jth spin is in the ground state, the Hamiltonian (A7) reduces to

$$H_e=-\sum_{j=1}^{N}\frac{g_m^2}{\delta_m}\hat{a}^{\dagger}\hat{a}|0\rangle_j\langle 0|-\sum_{j=1}^{N}\frac{\lambda^2}{\delta_{om}}\hat{a}^{\dagger}\hat{a}\hat{b}^{\dagger}\hat{b}|0\rangle_j\langle 0|. \tag{A8}$$

Under the conditions of the weak excitations and the large N, one can map the spin operators to the bosonic operators by using the Holstein-Primakoff transformation [69,70]:

$$\begin{aligned}
\sum_{j=1}^{N}\tau_{10}^{j-}&=\hat{c}\sqrt{N-\hat{c}^{\dagger}\hat{c}}\simeq\sqrt{N}\hat{c},\\
\sum_{j=1}^{N}\tau_{10}^{j+}&=\hat{c}^{\dagger}\sqrt{N-\hat{c}^{\dagger}\hat{c}}\simeq\sqrt{N}\hat{c}^{\dagger},
\end{aligned} \tag{A9}$$

where $\hat{c}^{\dagger}$ and $\hat{c}$ are bosonic operators which approximately obey the boson commutation relation $[\hat{c},\hat{c}^{\dagger}]\approx 1$ [71].

According to Eqs. (A9), one has $\sum_{j=1}^{N}|0\rangle_j\langle 0|=\sum_{j=1}^{N}\tau_{10}^{j-}\tau_{10}^{j+}\simeq N\hat{c}\hat{c}^{\dagger}$. Therefore, the Hamiltonian (A8) can be further rewritten as

$$\begin{aligned}H_e &= -\frac{(\sqrt{N}g_m)^2}{\delta_m}\hat{a}^\dagger\hat{a}\hat{c}\hat{c}^\dagger - \frac{(\sqrt{N}\lambda)^2}{\delta_{om}}\hat{a}^\dagger\hat{a}\hat{b}^\dagger\hat{b}\hat{c}\hat{c}^\dagger \\ &= -\lambda_m\hat{a}^\dagger\hat{a} - \chi\hat{a}^\dagger\hat{a}\hat{b}^\dagger\hat{b} \\ &\quad -\lambda_m\hat{a}^\dagger\hat{a}\hat{c}^\dagger\hat{c} - \chi\hat{a}^\dagger\hat{a}\hat{b}^\dagger\hat{b}\hat{c}^\dagger\hat{c},\end{aligned} \tag{A10}$$

where $\lambda_m = (\sqrt{N}g_m)^2/\delta_m$ and $\chi = (\sqrt{N}\lambda)^2/\delta_{om}$.

When the spin ensemble is in the ground state $|0\rangle_c$, the interactions described by last line of Eqs. (A10) can be neglected. Thus, the Hamiltonian (A10) becomes

$$H_e = -\lambda_m\hat{a}^\dagger\hat{a} - \chi\hat{a}^\dagger\hat{a}\hat{b}^\dagger\hat{b}. \tag{A11}$$

In a rotating frame under the Hamiltonian $H_0 = -\lambda_m\hat{a}^\dagger\hat{a}$, one has

$$H_e = e^{iH_0t}(-\chi\hat{a}^\dagger\hat{a}\hat{b}^\dagger\hat{b})e^{-iH_0t} = -\chi\hat{a}^\dagger\hat{a}\hat{b}^\dagger\hat{b}, \tag{A12}$$

which is the Hamiltonian (7) in the main text.

[1] Z. L. Xiang, S. Ashhab, J. Q. You, and F. Nori, Hybrid quantum circuits: Superconducting circuits interacting with other quantum systems, Rev. Mod. Phys. **85**, 623 (2013).

[2] G. Kurizki, P. Bertet, Y. Kubo, K. Mørlmer, D. Petrosyan, P. Rabl, and J. Schmiedmayer, Quantum technologies with hybrid systems, Proc. Natl. Acad. Sci. USA **112**, 3866 (2015).

[3] A. A. Clerk, K. W. Lehnert, P. Bertet, J. R. Petta, and Y. Nakamura, Hybrid quantum systems with circuit quantum electrodynamics, Nat. Phys. **16**, 257 (2020).

[4] I. Lekavicius, D. Andrew Golter, T. Oo, and H. Wang, Transfer of phase information between microwave and optical fields via an electron spin, Phys. Rev. Lett. **119**, 063601 (2017).

[5] B. Li, P. B. Li, Y. Zhou, S. L. Ma, and F. L. Li, Quantum microwave-optical interface with nitrogen-vacancy centers in diamond, Phys. Rev. A **96**, 032342 (2017).

[6] T. Liu, J. L. Zhao, B. Q. Guo, Q. C. Wu, Y. H. Zhou, and C. P. Yang, One-step implementation of a coherent conversion between microwave and optical cavities via an ensemble of nitrogen-vacancy centers, Phys. Rev. A **103**, 023706 (2021).

[7] Y. Kubo, F. R. Ong, P. Bertet, D. Vion, V. Jacques, D. Zheng, A. Dréau, J. F. Roch, A. Auffeves, F. Jelezko, J. Wrachtrup, M. F. Barthe, P. Bergonzo, and D. Esteve, Strong coupling of a spin ensemble to a superconducting resonator, Phys. Rev. Lett. **105**, 140502 (2010).

[8] R. Amsüss, Ch. Koller, T. Nöbauer, S. Putz, S. Rotter, K. Sandner, S. Schneider, M. Schramböck, G. Steinhauser, H. Ritsch, J. Schmiedmayer, and J. Majer, Cavity QED with magnetically coupled collective spin states, Phys. Rev. Lett. **107**, 060502 (2011).

[9] B. Julsgaard, C. Grezes, P. Bertet, and K. Mølmer, Quantum memory for microwave photons in an inhomogeneously broadened spin ensemble, Phys. Rev. Lett. **110**, 250503 (2013).

[10] S. Putz, D. O. Krimer, R. Amsüss, A. Valookaran, T. Nöbauer, J. Schmiedmayer, S. Rotter, and J. Majer, Protecting a spin ensemble against decoherence in the strong-coupling regime of cavity QED, Nat. Phys. **10**, 720 (2014).

[11] Y. S. Park, A. K. Cook, and H. Wang, Cavity QED with diamond nanocrystals and silica microspheres, Nano Lett. **6**, 2075 (2006).

[12] S. Schietinger, T. Schröder, and O. Benson, One-by-one coupling of single defect centers in nanodiamonds to high-Q modes of an optical microresonator, Nano Lett. **8**, 3911 (2008).

[13] P. E. Barclay, K. M. C. Fu, C. Santori, and R. G. Beausoleil, Chip-based microcavities coupled to nitrogen-vacancy centers in single crystal diamond, Appl. Phys. Lett. **95**, 191115 (2009).

[14] P. E. Barclay, C. Santori, K. M. Fu, R. G. Beausoleil, and O. Painter, Coherent interference effects in a nano-assembled diamond NV center cavity-QED system, Opt. Express **17**, 8081 (2009).

[15] X. Zhu, S. Saito, A. Kemp, K. Kakuyanagi, S. Karimoto, H. Nakano, W. J. Munro, Y. Tokura, M. S. Everitt, K. Nemoto, M. Kasu, N. Mizuochi, and K. Semba, Coherent coupling of a superconducting flux qubit to an electron spin ensemble in diamond, Nature (London) **478**, 221 (2011).

[16] J. H. Wesenberg, A. Ardavan, G. A. D. Briggs, J. J. L. Morton, R. J. Schoelkopf, D. I. Schuster, and K. Mølmer, Quantum computing with an electron spin ensemble, Phys. Rev. Lett. **103**, 070502 (2009).

[17] D. Marcos, M. Wubs, J. M. Taylor, R. Aguado, M. D. Lukin, and A. S. Sørensen, Coupling nitrogen-vacancy centers in diamond to superconducting flux qubits, Phys. Rev. Lett. **105**, 210501 (2010).

[18] W. L. Yang, Y. Hu, Z. Q. Yin, Z. J. Deng, and M. Feng, Entanglement of nitrogen-vacancy-center ensembles using transmission line resonators and a superconducting phase qubit, Phys. Rev. A **83**, 022302 (2011).

[19] Z. L. Xiang, X. Y. Lü, T. F. Li, J. Q. You, and F. Nori, Hybrid quantum circuit consisting of a superconducting flux qubit coupled to a spin ensemble and a transmission-line resonator, Phys. Rev. B **87**, 144516 (2013).

[20] X. Y. Lü, Z. L. Xiang, W. Cui, J. Q. You, and F. Nori, Quantum memory using a hybrid circuit with flux qubits and nitrogen-vacancy centers, Phys. Rev. A **88**, 012329 (2013).

[21] L. J. Zou, D. Marcos, S. Diehl, S. Putz, J. Schmiedmayer, J. Majer, and P. Rabl, Implementation of the Dicke lattice model in hybrid quantum system arrays, Phys. Rev. Lett. **113**, 023603 (2014).

[22] T. Liu, Q. P. Su, S. J. Xiong, J. M. Liu, C. P. Yang, and F. Nori, Generation of a macroscopic entangled coherent state using quantum memories in circuit QED, Sci. Rep. **6**, 32004 (2016).

[23] T. Liu, B. Q. Guo, C. S. Yu, and W. N. Zhang, One-step implementation of a hybrid Fredkin gate with quantum memories and single superconducting qubit in circuit QED and its applications, Opt. Express **26**, 4498 (2018).

[24] F. Y. Zhang and C. P. Yang, Tunable coupling of spin ensembles, Opt. Lett. **43**, 466 (2018).

[25] Y. Maleki and A. M. Zheltikov, Witnessing quantum entanglement in ensembles of nitrogen-vacancy centers coupled to a superconducting resonator, Opt. Express **26**, 17849 (2018).

[26] S. L. Ma, X. K. Li, J. K. Xie, and F. L. Li, Two-mode squeezed states of two separated nitrogen-vacancy-center ensembles

coupled via dissipative photons of superconducting resonators, Phys. Rev. A **99**, 012325 (2019).

[27] Y. Zhang, Q. Wu, S. L. Su, Q. Lou, C. Shan, and K. Mølmer, Cavity quantum electrodynamics effects with nitrogen vacancy center spins coupled to room temperature microwave resonators, Phys. Rev. Lett. **128**, 253601 (2022).

[28] J. Xu and T. Liu, Transfer of arbitrary quantum states between separated superconducting cavities via an ensemble of nitrogen-vacancy centers, Res. Phys. **44**, 106157 (2023).

[29] T. Liu, J. Xu, Y. Zhang, Y. Yu, Q. P. Su, Y. H. Zhou, and C. P. Yang, Efficient scheme for implementing a hybrid Toffoli gate with two NV ensembles simultaneously controlling a single superconducting qubit, Appl. Phys. Lett. **123**, 134002 (2023).

[30] D. Vitali, M. Fortunato, and P. Tombesi, Complete quantum teleportation with a Kerr nonlinearity, Phys. Rev. Lett. **85**, 445 (2000).

[31] N. Imoto, H. A. Haus, and Y. Yamamoto, Quantum nondemolition measurement of the photon number via the optical Kerr effect, Phys. Rev. A **32**, 2287 (1985).

[32] Y. B. Sheng, F. G. Deng, and H. Y. Zhou, Efficient polarization-entanglement purification based on parametric down-conversion sources with cross-Kerr nonlinearity, Phys. Rev. A **77**, 042308 (2008).

[33] D. J. Brod and J. Combes, Passive CPHASE gate via cross-Kerr nonlinearities, Phys. Rev. Lett. **117**, 080502 (2016).

[34] T. Liu, Y. Zhang, B. Q. Guo, C. S. Yu, and W. N. Zhang, Circuit QED: Cross-Kerr effect induced by a superconducting qutrit without classical pulses, Quantum Inf. Process. **16**, 209 (2017).

[35] K. Fukui, M. Endo, W. Asavanant, A. Sakaguchi, J. Yoshikawa, and A. Furusawa, Generating the Gottesman-Kitaev-Preskill qubit using a cross-Kerr interaction between squeezed light and Fock states in optics, Phys. Rev. A **105**, 022436 (2022).

[36] H. Schmidt and A. Imamoglu, Giant Kerr nonlinearities obtained by electromagnetically induced transparency, Opt. Lett. **21**, 1936 (1996).

[37] G. F. Sinclair and N. Korolkova, Cross-Kerr interaction in a four-level atomic system, Phys. Rev. A **76**, 033803 (2007).

[38] F. L. Semião and A. V. Barranco, Effective cross-Kerr nonlinearity and robust phase gates with trapped ions, Phys. Rev. A **72**, 064305 (2005).

[39] Z. R. Gong, H. Ian, Y. Liu, C. P. Sun, and F. Nori, Effective Hamiltonian approach to the Kerr nonlinearity in an optomechanical system, Phys. Rev. A **80**, 065801 (2009).

[40] J. Q. Liao, J. F. Huang, L. Tian, L. M. Kuang, and C. P. Sun, Generalized ultrastrong optomechanical-like coupling, Phys. Rev. A **101**, 063802 (2020).

[41] T. Opatrný and D. G. Welsch, Coupled cavities for enhancing the cross-phase-modulation in electromagnetically induced transparency, Phys. Rev. A **64**, 023805 (2001).

[42] L. Dao-Ming and Z. Shi-Biao, Scheme for realizing Kerr nonlinearity in cavity QED, Chin. Phys. Lett. **24**, 1567 (2007).

[43] Y. Hu, G. Q. Ge, S. Chen, X. F. Yang, and Y. L. Chen, Cross-Kerr-effect induced by coupled Josephson qubits in circuit quantum electrodynamics, Phys. Rev. A **84**, 012329 (2011).

[44] A. F. Kockum, A. Miranowicz, V. Macrì, S. Savasta, and F. Nori, Deterministic quantum nonlinear optics with single atoms and virtual photons, Phys. Rev. A **95**, 063849 (2017).

[45] H. Kang and Y. Zhu, Observation of large Kerr nonlinearity at low light intensities, Phys. Rev. Lett. **93**, 073601 (2004).

[46] J. Sinclair, D. Angulo, N. Lupu-Gladstein, K. Bonsma-Fisher, and A. M. Steinberg, Observation of a large, resonant, cross-Kerr nonlinearity in a cold Rydberg gas, Phys. Rev. Res. **1**, 033193 (2019).

[47] B. Fan, A. F. Kockum, J. Combes, G. Johansson, I. Hoi, C. M. Wilson, P. Delsing, G. J. Milburn, and T. M. Stace, Breakdown of the cross-Kerr scheme for photon counting, Phys. Rev. Lett. **110**, 053601 (2013).

[48] I. Hoi, A. F. Kockum, T. Palomaki, T. M. Stace, B. Fan, L. Tornberg, S. R. Sathyamoorthy, G. Johansson, P. Delsing, and C. M. Wilson, Giant cross-Kerr effect for propagating microwaves induced by an artificial atom, Phys. Rev. Lett. **111**, 053601 (2013).

[49] M. Kounalakis, C. Dickel, A. Bruno, N. K. Langford, and G. A. Steele, Tuneable hopping and nonlinear cross-Kerr interactions in a high-coherence superconducting circuit, npj Quantum Inf. **4**, 38 (2018).

[50] S. Ding, G. Maslennikov, R. Hablützel, and D. Matsukevich, Cross-Kerr nonlinearity for phonon counting, Phys. Rev. Lett. **119**, 193602 (2017).

[51] W. J. Wu, D. Xu, J. Qian, J. Li, Y. P. Wang, and J. Q. You, Observation of magnon cross-Kerr effect in cavity magnonics, arXiv:2112.13807.

[52] P. van Loock, Optical hybrid approaches to quantum information, Laser Photonics Rev. **5**, 167 (2011).

[53] U. L. Andersen, J. S. N. Nielsen, P. van Loock, and A. Furusawa, Hybrid discrete-and continuous-variable quantum information, Nat. Phys. **11**, 713 (2015).

[54] H. Jeong, Using weak nonlinearity under decoherence for macroscopic entanglement generation and quantum computation, Phys. Rev. A **72**, 034305 (2005).

[55] S. H. Xiang and K. H. Song, Non-Gaussian correlation estimates of two-mode hybrid entangled states via cross-Kerr medium and cumulant method, Eur. Phys. J. D **72**, 185 (2018).

[56] Y. Zhang, T. Liu, J. Zhao, Y. Yu, and C. P. Yang, Generation of hybrid Greenberger-Horne-Zeilinger entangled states of particlelike and wavelike optical qubits in circuit QED, Phys. Rev. A **101**, 062334 (2020).

[57] Q. P. Su, T. Liu, Y. Zhang, and C. P. Yang, Construction of a qudit using Schrödinger cat states and generation of hybrid entanglement between a discrete-variable qudit and a continuous-variable qudit, Phys. Rev. A **104**, 032412 (2021).

[58] H. Jeong, A. Zavatta, M. Kang, S. W. Lee, L. S. Costanzo, S. Grandi, T. C. Ralph, and M. Bellini, Generation of hybrid entanglement of light, Nat. Photon. **8**, 564 (2014).

[59] O. Morin, K. Huang, J. Liu, H. L. Jeannic, C. Fabre, and J. Laurat, Remote creation of hybrid entanglement between particle-like and wave-like optical qubits, Nat. Photon. **8**, 570 (2014).

[60] K. Huang, H. L. Jeannic, O. Morin, T. Darras, G. Guccione, A. Cavaillès, and J. Laurat, Engineering optical hybrid entanglement between discrete- and continuous-variable states, New J. Phys. **21**, 083033 (2019).

[61] R. Hisatomi, A. Osada, Y. Tabuchi, T. Ishikawa, A. Noguchi, R. Yamazaki, K. Usami, and Y. Nakamura, Bidirectional conversion between microwave and light via ferromagnetic magnons, Phys. Rev. B **93**, 174427 (2016).

[62] L. A. Williamson, Y. H. Chen, and J. J. Longdell, Magneto-optic modulator with unit quantum efficiency, Phys. Rev. Lett. **113**, 203601 (2014).

[63] J. Rochman, T. Xie, J. G. Bartholomew, K. C. Schwab, and A. Faraon, Microwave-to-optical transduction with erbium ions coupled to planar photonic and superconducting resonators, Nat. Commun. **14**, 1153 (2023).

[64] C. Weinzetl, J. Görlitz, J. N. Becker, I. A. Walmsley, E. Poem, J. Nunn, and C. Becher, Coherent control and wave mixing in an ensemble of silicon-vacancy centers in diamond, Phys. Rev. Lett. **122**, 063601 (2019).

[65] E. Togan, Y. Chu, A. S. Trifonov, L. Jiang, J. Maze, L. Childress, M. V. G. Dutt, A. S. Sørensen, P. R. Hemmer, A. S. Zibrov, and M. D. Lukin, Quantum entanglement between an optical photon and a solid-state spin qubit, Nature (London) **466**, 730 (2010).

[66] S. B. Zheng and G. C. Guo, Efficient scheme for two-atom entanglement and quantum information processing in cavity QED, Phys. Rev. Lett. **85**, 2392 (2000).

[67] D. F. V. James, Quantum computation with hot and cold ions: An assessment of proposed schemes, Fortschr. Phys. **48**, 823 (2000).

[68] D. F. James and J. Jerke, Effective Hamiltonian theory and its applications in quantum information, Can. J. Phys. **85**, 625 (2007).

[69] T. Holstein and H. Primakoff, Field dependence of the intrinsic domain magnetization of a ferromagnet, Phys. Rev. **58**, 1098 (1940).

[70] K. Hammerer, A. S. Sørensen, and E. S. Polzik, Quantum interface between light and atomic ensembles, Rev. Mod. Phys. **82**, 1041 (2010).

[71] Y. X. Liu, C. P. Sun, S. X. Yu, and D. L. Zhou, Semiconductor-cavity QED in high-Q regimes with q-deformed bosons, Phys. Rev. A **63**, 023802 (2001).

[72] J. R. Johansson, P. D. Nation, and F. Nori, QuTiP: An open source python framework for the dynamics of open quantum systems, Comput. Phys. Commun. **183**, 1760 (2012).

[73] J. R. Johansson, P. D. Nation, and F. Nori, QuTiP 2: A Python framework for the dynamics of open quantum systems, Comput. Phys. Commun. **184**, 1234 (2013).

[74] T. Nöbauer, K. Buczak, A. Angerer, S. Putz, G. Steinhauser, J. Akbarzadeh, H. Peterlik, J. Majer, J. Schmiedmayer, and M. Trupke, Creation of ensembles of nitrogen-vacancy centers in diamond by neutron and electron irradiation, arXiv:1309.0453.

[75] K. Sandner, H. Ritsch, R. Amsüss, C. Koller, T. Nöbauer, S. Putz, J. Schmiedmayer, and J. Majer, Strong magnetic coupling of an inhomogeneous nitrogen-vacancy ensemble to a cavity, Phys. Rev. A **85**, 053806 (2012).

[76] H. Bernien, L. Childress, L. Robledo, M. Markham, D. Twitchen, and R. Hanson, Two-photon quantum interference from separate nitrogen vacancy centers in diamond, Phys. Rev. Lett. **108**, 043604 (2012).

[77] C. Santori, D. Fattal, S. M. Spillane, M. Fiorentino, R. G. Beausoleil, A. D. Greentree, P. Olivero, M. Draganski, J. R. Rabeau, P. Reichart, B. C. Gibson, S. Rubanov, D. N. Jamieson, and S. Prawer, Coherent population trapping in diamond N-V centers at zero magnetic field, Opt. Express **14**, 7986 (2006).

[78] C. Santori, P. E. Barclay, K. C. Fu, R. G. Beausoleil, S. Spillane, and M. Fisch, Nanophotonics for quantum optics using nitrogen-vacancy centers in diamond, Nanotechnol. **21**, 274008 (2010).

[79] A. Megrant, C. Neill, R. Barends, B. Chiaro, Y. Chen, L. Feigl, J. Kelly, E. Lucero, M. Mariantoni, P. J. J. O'Malley, D. Sank, A. Vainsencher, J. Wenner, T. C. White, Y. Yin, J. Zhao, C. J. Palmstrøm, J. M. Martinis, and A. N. Cleland, Planar superconducting resonators with internal quality factors above one million, Appl. Phys. Lett. **100**, 113510 (2012).

[80] A. A. Savchenkov, A. B. Matsko, V. S. Ilchenko, and L. Maleki, Optical resonators with ten million finesse, Opt. Express **15**, 6768 (2007).

[81] V. Huet, A. Rasoloniaina, P. Guillemé, P. Rochard, P. Féron, M. Mortier, A. Levenson, K. Bencheikh, A. Yacomotti, and Y. Dumeige, Millisecond photon lifetime in a slow-light microcavity, Phys. Rev. Lett. **116**, 133902 (2016).

[82] P. L. Stanwix, L. M. Pham, J. R. Maze, D. Le Sage, T. K. Yeung, P. Cappellaro, P. R. Hemmer, A. Yacoby, M. D. Lukin, and R. L. Walsworth, Coherence of nitrogen-vacancy electronic spin ensembles in diamond, Phys. Rev. B **82**, 201201(R) (2010).

[83] N. Bar-Gill, L. M. Pham, A. Jarmola, D. Budker, and R. L. Walsworth, Solid-state electronic spin coherence time approaching one second, Nat. Commun. **4**, 1743 (2013).

[84] G. Calusine, A. Melville, W. Woods, R. Das, C. Stull, V. Bolkhovsky, D. Braje, D. Hover, D. K. Kim, X. Miloshi, D. Rosenberg, A. Sevi, J. L. Yoder, E. Dauler, and W. D. Oliver, Analysis and mitigation of interface losses in trenched superconducting coplanar waveguide resonators, Appl. Phys. Lett. **112**, 062601 (2018).

[85] I. S. Grudinin, V. S. Ilchenko, and L. Maleki, Ultrahigh optical Q factors of crystalline resonators in the linear regime, Phys. Rev. A **74**, 063806 (2006).

[86] T. Aoki, B. Dayan, E. Wilcut, W. P. Bowen, A. S. Parkins, T. J. Kippenberg, K. J. Vahala, and H. J. Kimble, Observation of strong coupling between one atom and a monolithic microresonator, Nature (London) **443**, 671 (2006).